



Article

Asymmetric Magneto-Optical Rotation in Magnetoplasmonic Nanocomposites

Sergey Tomilin ^{1,*}, Andrey Karavaynikov ¹ , Sergey Lyashko ¹, Olga Tomilina ¹, Vladimir Berzhansky ¹, Alexey Gusev ¹, Wolfgang Linert ² and Alexander Yanovsky ³

¹ Institute of Physics and Technology, V.I. Vernadsky Crimean Federal University, Vernadsky Avenue, 4, Simferopol 295007, Russia; domain@cfuv.ru (A.K.); 0jmaster0@gmail.com (S.L.); olga_tomilina@mail.ru (O.T.); v.n.berzhansky@gmail.com (V.B.); galex0330@gmail.com (A.G.)

² Institute of Applied Physics, Vienna University of Technology, Wiedner Hauptstraße 8–10, 1040 Vienna, Austria; wolfgang.linert@tuwien.ac.at

³ Faculty of Mathematics, Zaporizhzhya National University, Zhukovcky Str., 66, 69600 Zaporizhzhya, Ukraine; yanovskiyas@gmail.com

* Correspondence: tomlin_znu@mail.ru

Abstract: The results of the asymmetric magneto-optical rotation in the magnetoplasmonic nanocomposite study are presented. The asymmetry is observed in spectra of magneto-optical rotation when a magneto-optical medium with a plasmonic subsystem is magnetized along or against the radiation wave vector. The asymmetry is observed as vertical displacement of a magneto-optical hysteresis loop too. Such asymmetry is detected in magnetoplasmonic nanocomposite, which consists of a magneto-optical layer of Bi substituted iron-garnet intercalated with a plasmonic subsystem of gold self-assembled nanoparticles. It is shown that the physical reason for the asymmetric magneto-optical rotation is the manifestation of the Cotton–Mouton birefringence effect when the normal magnetization of the sample to a radiation wave vector appears due to the magnetic component of the electromagnetic field of resonating nanoparticles. This effect is additive to the basic magneto-optical Faraday Effect.

Keywords: vacuum deposition; thin film; thermal activated granulation; nanoparticles; plasmonic resonance; iron-garnet; Faraday Effect; magnetoplasmonic nanocomposite



Citation: Tomilin, S.; Karavaynikov, A.; Lyashko, S.; Tomilina, O.; Berzhansky, V.; Gusev, A.; Linert, W.; Yanovsky, A. Asymmetric Magneto-Optical Rotation in Magnetoplasmonic Nanocomposites. *J. Compos. Sci.* **2023**, *7*, 287. <https://doi.org/10.3390/jcs7070287>

Academic Editor: Francesco Tornabene

Received: 12 May 2023

Revised: 24 June 2023

Accepted: 11 July 2023

Published: 13 July 2023



Copyright: © 2023 by the authors. Licensee MDPI, Basel, Switzerland. This article is an open access article distributed under the terms and conditions of the Creative Commons Attribution (CC BY) license (<https://creativecommons.org/licenses/by/4.0/>).

1. Introduction

The new trends of miniaturization and quantum technology stimulate the synthesis and investigation of nanosized elements, structures, and composites with various properties in the range of optics, magnetics, magneto-optics, plasmonics, etc. It led to the creation of such areas as nanophotonics, magneto-photonics, plasmonic nanosensorics, magnonics, and spintronics. Magnetoplasmonics arose as a result of intersected research in the study of metals plasmonics and magneto-optics of transparent magneto-dielectric materials [1,2]. Using bismuth-substituted iron-garnets (BiIG) as the magneto-optical materials is advantageous due to their high magneto-optical quality factor. The BiIG films have relatively low absorption and significant magnitudes of magneto-optical effects.

It has been shown that the magneto-optical effects in magnetic iron-garnet films are very valuable in different applications of photonics, spintronics, sensorics, magnetometry, etc. [3–5]. In order to enhance the magneto-optical effect for these applications, various methods can be used. A large number of works are dedicated to the study of the enhancement of light polarization rotation in iron-garnets (Faraday Effect) due to the addition of a plasmonic subsystem of self-assembled or ordered metal nanoparticles [6–12]. The resonance excitation of collective oscillations of free electrons (electronic plasma) in metal nanoparticles leads to the appearance of localized plasmonic modes (localized plasmonic resonances, LPR) [13–15]. The spectral position of these modes is determined by the size,

shape, and dielectric environment of plasmonic nanoparticles. Depending on the size factors (shape, diameter, aspect ratio), various LPR modes can be excited in plasmonic nanoparticles. These can be modes of oscillations (dipole, quadrupole, octupole, hexadecapole, etc.), dimensional modes in spherically nonsymmetric and irregularly shaped nanoparticles (for example, longitudinal and transverse modes in nanorods), or modes of coupled oscillations (for example, as a result of dipole–dipole interaction between neighbor nanoparticles) [16–19].

At the LPR resonant condition, a significant increase in the electromagnetic field is observed in the vicinity of the resonated plasmonic subsystem. It leads to near-field interaction between plasmonic and magnetic subsystems and enhancement of the magneto-optical Faraday Effect. A similar enhancement of the Faraday rotation in magnetoplasmonic nanocomposites was also studied by us recently [20,21]. The unambiguously physical nature of such plasmonic enhancement of the Faraday Effect in magnetoplasmonic composites has not been established. So, the authors in the work [22] associated the increase in optical rotation with the plasmon absorption of the p-polarized component of the transmitted light relative to the incident light. On the other hand, such an increase in the magneto-optical polarization rotation can be described as a result of a magnetic circular dichroism enhancement as a result of an increase in the Zeeman splitting in the near field of a resonating plasmonic particle [23]. But the very fact of plasmonic enhancement of the magneto-optical Faraday Effect is confirmed experimentally and described in numerous publications.

In addition, the effect of the vertical shift of the magneto-optical hysteresis loop (MOHL) in the vicinity of localized plasmonic resonance (LPR) excited in the plasmonic subsystem was discovered [21,24]. This effect is not dependent on the external magnetic field and is observed as an additive term $\Delta\Theta$ to the magneto-optical hysteresis loop. At spectral investigations in a constant external magnetizing field, this effect of magneto-optical hysteresis loop vertical displacement manifests itself in the form of an asymmetry of the magneto-optical spectra of the Faraday rotation when the magnetoplasmonic nanocomposite is magnetized along or against the light wave vector.

A detailed study of this effect is of great interest both for fundamentals and for applications in spintronics, sensorics, magneto-optics, photonics, etc. [25–27]. The article deals with the study of the peculiarities of the asymmetric Faraday Effect during the various plasmon modes' interaction with the electronic structure of bismuth-substituted iron-garnet BiIG when the ratio of plasmonic Au particles diameter and the iron-garnet coating thickness is changed.

2. Samples Preparation and Characterization

For magnetoplasmonic nanocomposite manufacturing, self-assembled Au nanoparticles ($\text{Au}_{(\text{NP})}$) were synthesized on a substrate of gadolinium-gallium garnet monocrystal $\text{Gd}_3\text{Ga}_5\text{O}_{12}$ (GGG, "Istok", Fryazino, Russia). Nanoparticles were synthesized by thermal treatment of ultrathin gold film at 950 °C for 10 min [28]. A gold film with an effective thickness of $h_{\text{eff}} = 5$ nm has been obtained by thermal evaporation of Au (99.95%) in a vacuum. The pressure of residual gases was not more than 5×10^{-4} Pa. Figure 1a presents an SEM image of a GGG/ $\text{Au}_{(\text{NP})}$ sample surface (scanning electronic microscope is "REM-106 Selmi", Sumy, Ukraine, electron incidence angle is 45 deg to the sample surface). The detection at the angle of 45 deg allows one to analyze the spatial shape of plasmonic nanoparticles. As can be seen, the shape of Au self-assembled nanoparticles approaches an elliptical and resembles a "dew on a lotus leaf" (a drop of non-wetting liquid).

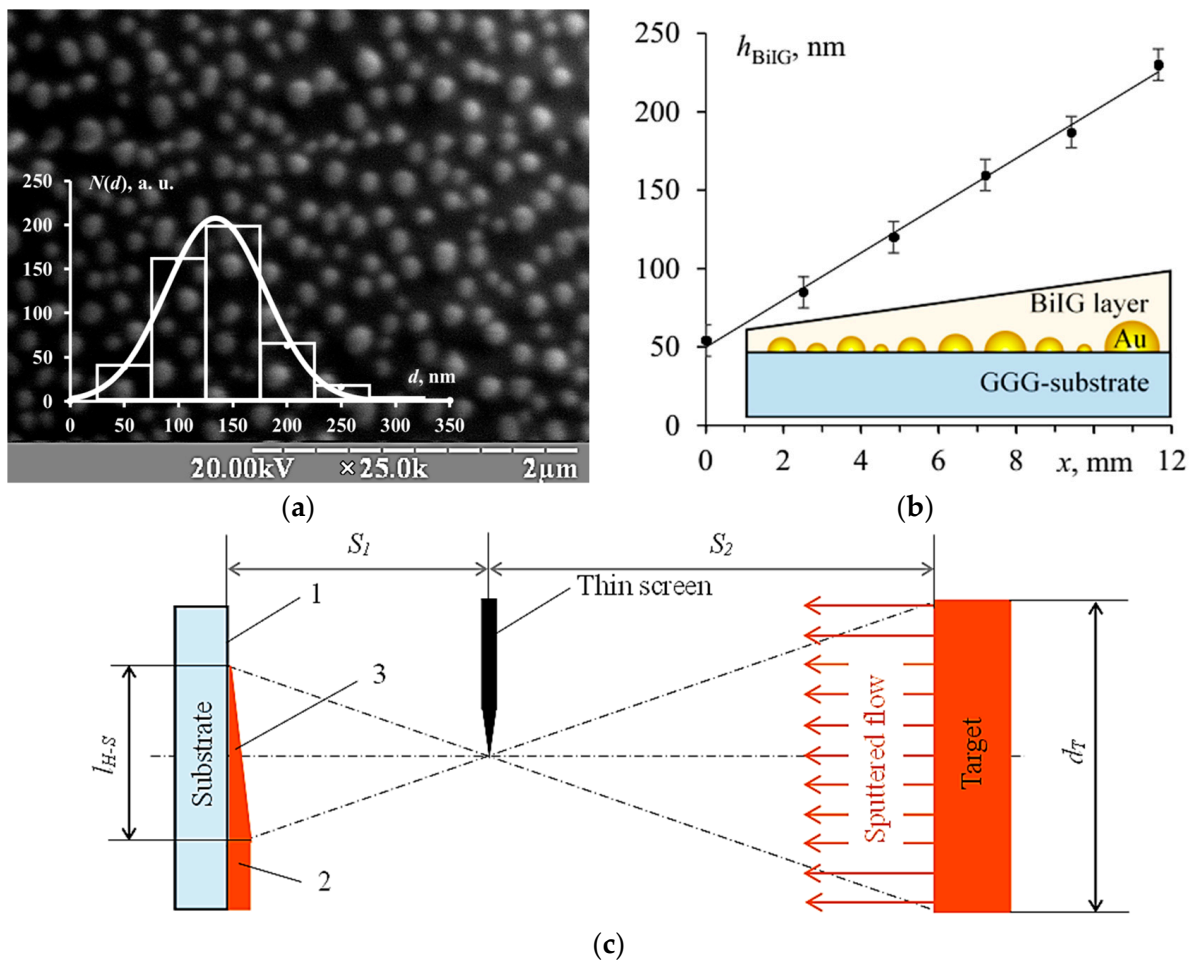


Figure 1. (a) SEM image of morphology of self-assembled gold nanoparticles, inset—size dispersion of Au nanoparticles (columns—experiment, curve—approximation by the Gaussian). (b) Change of garnet film thickness h_{BiIG} along the gradient, inset—the schematic structure of investigated nanocomposite GGG/Au_(NP)/BiIG_(grad h). (c) The scheme of a “half-shadow” technique for syntheses of gradient BiIG film.

The inset in Figure 1a shows the size dispersion of self-assembled gold nanoparticles. It can be seen that the dispersion of nanoparticles has a good approximation by the Gaussian function. In this case, the most probable diameter of $d_0 = 135$ nm and standard deviation of $\sigma = 45$ nm.

To obtain a magnetoplasmonic nanocomposite, a film of bismuth-substituted iron-garnet (BiIG) was deposited on the surface of Au nanoparticles. The stoichiometry composition of iron-garnet is $\text{Bi}_{2.0}\text{Gd}_{1.0}\text{Fe}_{3.8}\text{Al}_{1.2}\text{O}_{12}$. Deposition of the garnet layer was carried out using the ion-reactive sputtering of a target with an annular erosion zone. The iron-garnet target with a diameter of $d_T = 76$ mm was sputtered in a mixture of gases Ar (25%) + O₂ (75%) at a pressure of 10 Pa. The pressure of residual gases was not more than 5×10^{-4} Pa. The garnet film was annealed at 680 °C for 20 min in the air for crystallization. To obtain the sample with a thickness gradient of garnet film, a special coating deposition technique of “half-shadow” was used [24,28]. Figure 1c demonstrates the scheme of the “half-shadow” technique. A thin screen with a sharp straight edge was placed between the iron-garnet target and the substrate. This edge splits the sputtered flow and forms three zones on the substrate surface. Zone 1 is the pure substrate without film (covered by a screen), zone 2 is the coating with the maximal thickness (uncovered by a screen), and zone 3 (between 1 and 2) is the geometrical “half-shadow”. This “half-shadow” zone has a coating with a thickness gradient directed perpendicular to the sharp straight edge of the screen. The

length of the “half-shadow” zone can be changed by varying the ratio between the distance from the target to screen S_2 and the distance from screen to substrate S_1 . So, knowing the diameter of target d_T and parameters S_1 and S_2 , the length of the “half-shadow” zone l_{H-S} can be determined from the similarity of triangles.

The using of this “half-shadow” technique at the vacuum sputtering of iron-garnet allows one to obtain different thicknesses of the garnet matrix in different parts of the sample, which contains plasmonic nanoparticles. The investigation of plasmonic nanocomposite at different areas of a garnet thickness gradient makes it possible to study the features of its structural, optical, and magneto-optical properties at different ratios of the plasmonic nanoparticles size and the garnet matrix thickness.

The distribution of garnet film thickness along the gradient was investigated using a micro-interferometer (MII-4, “LOMO”, Saint-Petersburg, Russia) with a digital analysis unit. Figure 1b presents the distribution of the garnet layer thickness along a gradient. It has a good approximation by a linear function with an angular index of 15 nm/mm. The inset in Figure 1b shows the schematic structure (cross-section) of the obtained magnetoplasmonic nanocomposite $GGG/Au_{(NP)}/BiIG_{(grad\ h)}$.

The optical and magneto-optical characteristics of the synthesized nanocomposite $GGG/Au_{(NP)}/BiIG_{(grad\ h)}$ in different areas of the BiIG layer gradient were investigated using a spectral magneto-polarimeter based on a spectrophotometer (KFK-3, “ZOMZ”, Sergiev Pasad, Russia). Magneto-polarimeter has a monochromator with Czerny–Turner optical configuration and a magnetic cell with a polarizer–analyzer line. Magneto-optical properties of the nanocomposite were studied using the Faraday optical configuration. The angle of the polarization plane rotation was detected by a direct method of finding the transmission extremum in the crossed state of the polarizer and analyzer.

3. Results and Discussion

3.1. Optics and Plasmonics of Magnetoplasmonic Nanocomposite

The transmittance spectra of the plasmonic nanocomposite $GGG/Au_{(NP)}/BiIG_{(grad\ h)}$ at different areas of the gradient are shown in Figure 2a. The thickness of iron-garnet film h_{BiIG} in the investigated area is indicated in the legend.

The inset in Figure 2a shows the optical transmittance spectra of unannealed GGG/Au thin film and annealed $GGG/Au_{(NP)}$ self-assembled gold nanoparticles. As can be seen, the transmittance spectrum of $Au_{(NP)}$ nanoparticles exhibits a spectral trough. This trough is associated with the optical absorption for excitation of the LPR dipole mode (d -mode) in self-assembled gold nanoparticles [13,28–31]. In our case, the plasmonic system has a resonant wavelength of $\lambda_{LPR} = 660$ nm.

After deposition and annealing of a BiIG layer on the top of plasmonic nanoparticles, the LPR d -mode shifts to the infrared part of the spectrum. Also, a new local trough appears in the spectra. This trough is due to the resonant excitation of an additional “high-frequency” LPR mode [31].

As can be seen, both LPR modes have a significant “red” shift with an increase in garnet thickness [30,31]. In this case, the efficiency of the “high-frequency” mode excitation is increased, and the “low-frequency” dipole mode excitation is decreased. So, we can conclude that a new “high-frequency” mode emerges as a result of the dipole interaction between neighboring plasmon. The physical essence of this mode is the coupled dipole–dipole oscillations (d - d -mode), which was demonstrated earlier in [24,31].

Figure 2b shows the changes in the resonant wavelength along a gradient of the iron-garnet layer thickness for various LPR modes. It can be seen that when the garnet film (nanoparticles shell) thickness increases above 160 nm, the resonance spectral shift almost does not occur. It is due to the limited penetration depth of the field of localized plasmon oscillations into the magnetodielectric environment (near field). Thus, the interaction depth (near field penetration) of the resonating plasmonic subsystem with the magneto-optical BiIG matrix is realized at a distance not more than $h_{NF} = 2.5 \cdot r_{NP}$ [32], where r_{NP} is the radius of gold nanoparticles.

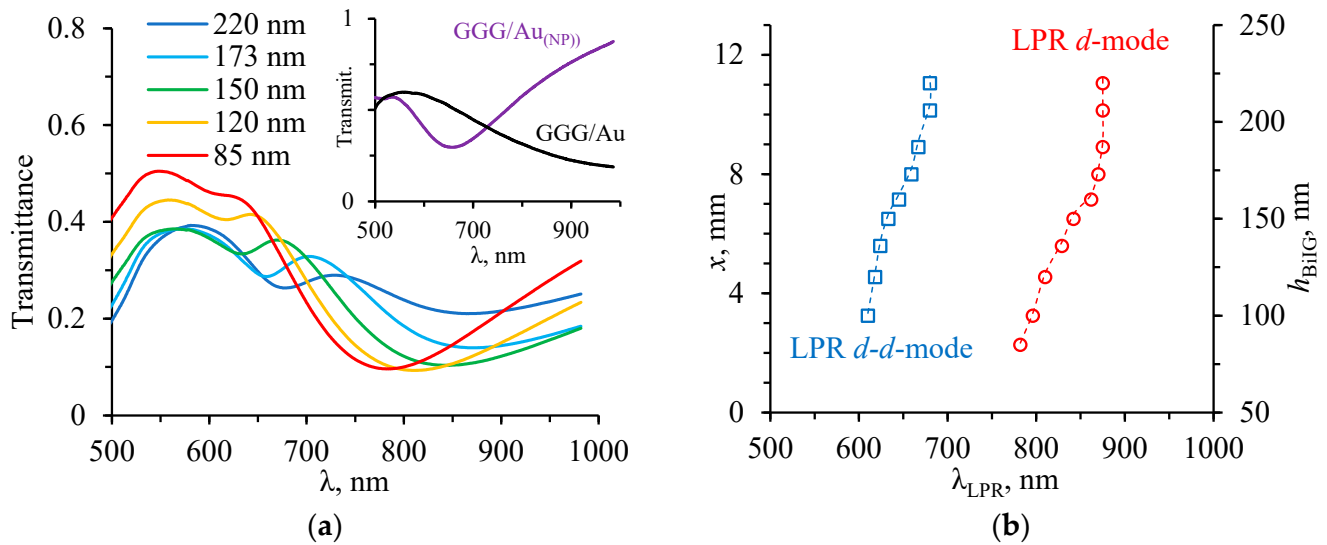


Figure 2. (a) Transmittance spectra of the GGG/Au_(NP)/BiIG_(grad h) nanocomposite at different thickness of the BiIG layer (h_{BiIG} is indicated in the legend), inset—transmittance spectra of a GGG/Au gold film (before annealing) and self-assembled GGG/Au_(NP) nanoparticles (after annealing); (b) the spectral position of various LPR modes along gradient at different thicknesses of garnet film h_{BiIG} [31].

3.2. Magneto-Optical Properties of Magnetoplasmonic Nanocomposite

The magneto-optical properties of the GGG/Au_(NP)/BiIG_(grad h) nanocomposite were investigated in Faraday configuration where the rotation angle Θ_{TR} of the light polarization was measured after passing through a sample magnetized to saturation (the external field of $H_0 = 170$ mT, the saturation field of $H_S \approx 80$ mT). The spectral measurements were carried out in the range of 460–980 nm. The magnetic field vector was oriented both along the radiation wave vector (field $H+$) and against it (field $H-$). Figure 3 shows the spectral features of magneto-optical rotation of the light polarization in fields $H+$ and $H-$ in different areas of gradient h_{BiIG} of the garnet film.

As can be seen from the figure, the magneto-optical rotation spectra of GGG/Au_(NP)/BiIG_(grad h) nanocomposite at $H+$ and $H-$ magnetization (Figure 3b–f) are not symmetric compared to a pure layer of GGG/BiIG garnet without a plasmon subsystem (Figure 3a). The more significant this asymmetry, the smaller the thickness of the iron-garnet layer. As shown above, this is due to the limited depth of the field penetration into the surrounding magnetodielectric from the resonating plasmonic nanoparticle. So, the effects associated with LPR in the plasmonic subsystem are more pronounced, with higher efficiency of the field interaction between the resonating particle and the garnet layer. Also, note that in the areas of the gradient with a small thickness of the BiIG layer, the rotation spectra in the fields $H+$ and $H-$ can intersect. An explanation of this effect will be given below in Section 3.3 based on the analysis of magneto-optical hysteresis loops (MOHLs).

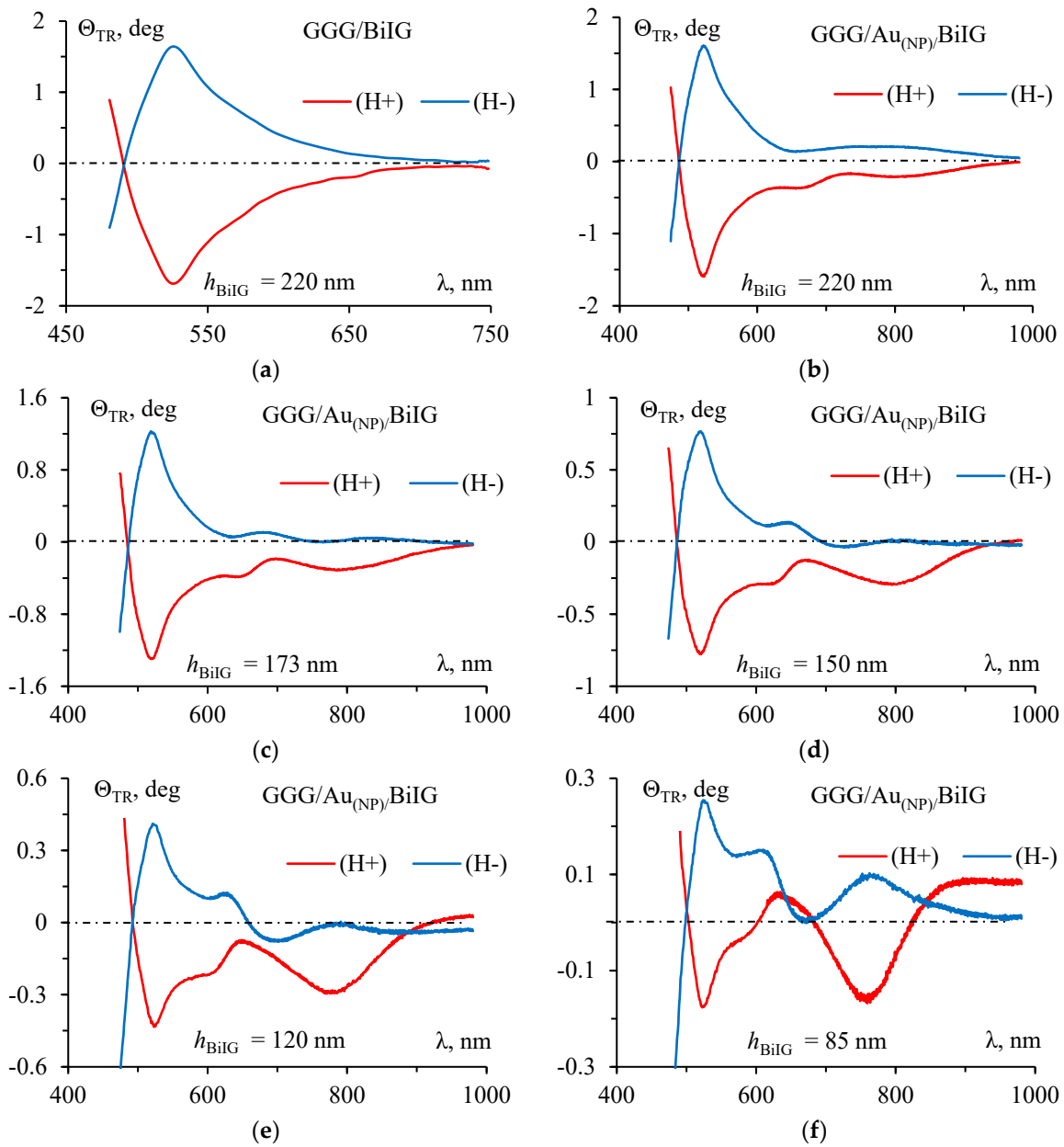


Figure 3. Magneto-optical rotation of the light polarization transmitted through 220 nm thick GGG/BiIG film without a plasmon subsystem (a) and through the GGG/Au_(NP)/BiIG_(grad h) nanocomposite at different values of the thickness h_{BiIG} : (b) 220 nm; (c) 173 nm; (d) 150 nm; (e) 120 nm; (f) 85 nm. Samples were magnetized along the wave vector ($H+$) and against it ($H-$).

As shown in [12,31], the Faraday rotation Θ_{FR} can be found directly as the half-height of the magneto-optical hysteresis loop or as half of the distance between the spectra of the total magneto-optical rotation $\Theta_{\text{TR}}(\lambda)$ in the fields $H+$ and $H-$, and is determined by the following expression:

$$\Theta_{\text{FR}}(\lambda) = \left[\Theta_{\text{TR}(H+)}(\lambda) - \Theta_{\text{TR}(H-)}(\lambda) \right] / 2 - \Theta_{\text{FR}(\text{GGG})}(\lambda) \quad (1)$$

And the asymmetry of magneto-optical rotation (vertical displacement of the magneto-optical loop)—as the shift of the middle of the loop or as the midline between the spectra of total rotation—is given by the following:

$$\Delta\Theta(\lambda) = \left[\Theta_{\text{TR}(H+)}(\lambda) + \Theta_{\text{TR}(H-)}(\lambda) \right] / 2 \quad (2)$$

Figure 4a shows the Faraday rotation spectra $\Theta_{FR}(\lambda)$, which were obtained using Equation (1) at different areas of the magneto-optical layer gradient h_{BiIG} in nanocomposite GGG/Au_(NP)/BiIG_(grad h).

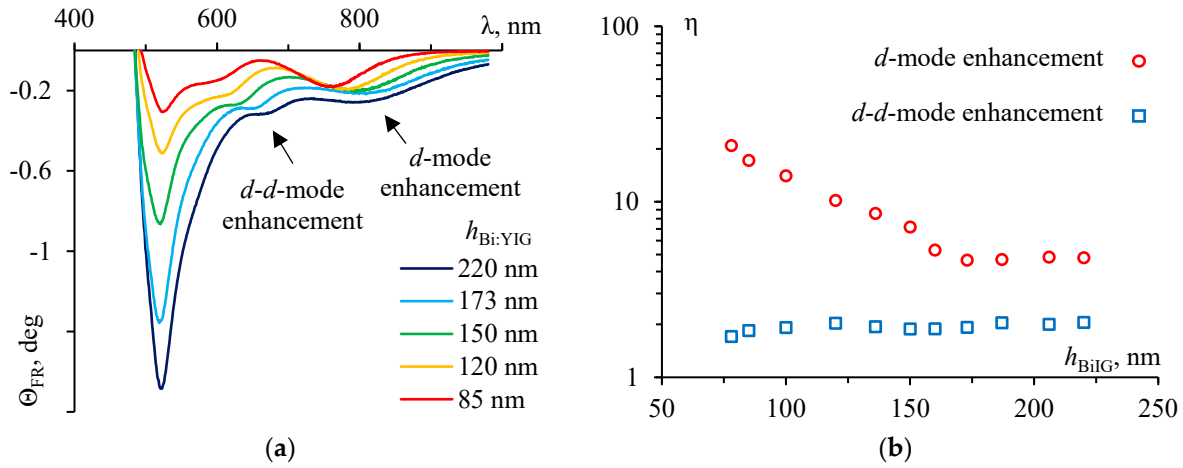


Figure 4. (a) Spectral features of Faraday Effect in the GGG/Au_(NP)/BiIG_(grad h) nanocomposite at different values of the BiIG layer thickness (h_{BiIG} is indicated in the legend); (b) Change of the factor η of the Faraday Effect enhancement as the function of the garnet layer thickness h_{BiIG} (due to different LPR modes) [31].

As seen in Figure 4a, an enhancement of the Faraday magneto-optical effect is observed in the spectral region of both LPR modes. To analyze this enhancement due to different modes, the factor of enhancement was calculated:

$$\eta = \frac{\Theta_{FR}(\lambda_{LPR})|_{GGG/Au(NP)/BiIG}}{\Theta_{FR}(\lambda_{LPR})|_{GGG/BiIG}} \tag{3}$$

Figure 4b shows the change of factor η of the Faraday Effect enhancement from both LPR modes depending on the thickness h_{BiIG} of the magneto-optical garnet film in the GGG/Au_(NP)/BiIG_(grad h) nanocomposite.

The enhancement η of the Faraday Effect due to the LPR *d*-mode increases significantly with a decrease in the BiIG layer thickness and reaches a value of more than 20 times. For the LPR *d-d*-mode, the Faraday Effect enhancement is less pronounced, and η is not above 1.5.

Let us analyze the value of the asymmetric magneto-optical rotation (AMOR) effect, which can be obtained from the total rotation spectra $\Theta_{TR}(\lambda)$ in $H+$ and $H-$ fields on the basis of Equation (2). Results of the analysis of the asymmetric magneto-optical rotation (magneto-optical hysteresis loop displacement) spectra $\Delta\Theta(\lambda)$ (Figure 5a) show that the greatest effect is observed in the vicinity of both LPR modes. In this case, the shift $\Delta\Theta$, as a rule, changes sign upon a spectral transition through the localized plasmonic resonance, and at the resonance itself $\Delta\Theta(\lambda_{LPR}) = 0$. But if several closely located resonance modes are present, an inflection point on the $\Delta\Theta(\lambda)$ curve at resonance is observed.

It has been revealed a correlation between the spectra of asymmetric magneto-optical rotation (magneto-optical hysteresis loop displacement) $\Delta\Theta(\lambda)$ and the spectra of the derivative of transmittance $dT/d\lambda(\lambda)$ (the position of the LPR resonance modes and the width of the resonance lines) [21]. For example, the comparison of spectral dependences $\Delta\Theta(\lambda)$ and $dT/d\lambda(\lambda)$ in the GGG/Au_(NP)/BiIG_(grad h) nanocomposite at a thickness $h_{BiIG} = 173$ nm is shown in Figure 5b. The spectral areas of the plasmonic *d-d*-mode of 660–670 nm) and *d*-mode of 870–880 nm

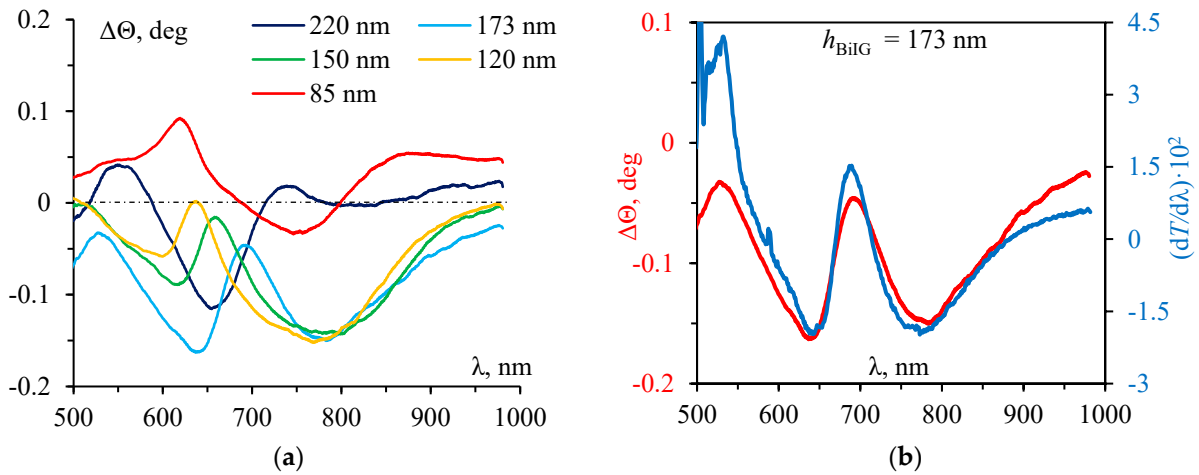


Figure 5. (a) Spectra of asymmetric magneto-optical rotation (magneto-optical hysteresis loop displacement) $\Delta\Theta(\lambda)$ in the magnetoplasmonic GGG/Au_(NP)/BiIG_(grad h) nanocomposite at different values of the magneto-optical layer thickness h_{BiIG} (indicated in the legend). (b) Graphical comparative analysis of the spectral dependences $\Delta\Theta(\lambda)$ and $dT/d\lambda(\lambda)$ obtained at a magnetic layer thickness $h_{\text{BiIG}} = 173$ nm.

Thus, the effect of asymmetric magneto-optical rotation (magneto-optical hysteresis loop displacement) is of a plasmonic nature, and the spectral dependence of the vertical displacement of the loop $\Delta\Theta(\lambda)$ is completely determined by the position and shape of the resonance lines of different LPR modes.

The physical meaning of asymmetric magneto-optical rotation (magneto-optical hysteresis loop displacement) is the manifestation of the Cotton–Mouton birefringence effect [33] when the magnetization of the sample in the direction normal to the radiation wave vector appears due to the magnetic component of the electromagnetic field of resonating nanoparticles. The change in the sign of $\Delta\Theta$ upon passing through the resonance point is due to the ratio of large and small plasmonic nanoparticles with respect to particles in resonance. It was previously shown in [21].

3.3. Analysis of Magneto-Optical Hysteresis Loops

As shown in Figure 2, at small BiIG layer thicknesses in GGG/Au_(NP)/BiIG_(grad h) (less than 150 nm), the spectral curves of magneto-optical rotation in fields $H+$ and $H-$ can intersect. To explain this fact, we have investigated magneto-optical hysteresis loops $\Theta_{\text{TR}}(H)$ for GGG/Au_(NP)/BiIG_(grad h) sample at the iron-garnet layer thickness $h_{\text{BiIG}} = 90$ nm (Figure 6).

Figure 6a presents the spectra of magneto-optical rotation of the polarization plane upon sample magnetization in fields $H+$ and $H-$; dashed lines and numbers show the spectral regions in which the magneto-optical hysteresis loop was studied, namely, $\lambda = 640$ nm—near the LPR $d-d$ -mode, $\lambda = 750$ nm—near the LPR d -mode, and $\lambda = 920$ nm—at the intersection of the curves $\Theta_{\text{TR}(H+)}(\lambda)$ and $\Theta_{\text{TR}(H-)}(\lambda)$.

The inset to Figure 6a shows the corresponding form of the magneto-optical hysteresis loop at sample magnetization reversal in the field $H = \pm 170$ mT. As can be seen from the figure, the shape of the magneto-optical hysteresis loop has a deformation, and the linear sections above the saturation field have a “negative” slope. The greatest deformation is observed for the magneto-optical hysteresis loop, which was obtained at $\lambda = 920$ nm (in the maximum field, the magnitude of deformation exceeds the height of the loop itself). To analyze the nature and magnitude of the deformation and restore the “true” shape of the magneto-optical hysteresis loop $\Theta_i'(H)$, a “fitting” straight line $k \cdot H + \Delta\Theta$ was subtracted from the experimental dependence $\Theta_i(H)$. Figure 6b–d show the corresponding “fitting” straight lines and their equations, as well as the form of magneto-optical hysteresis loop $\Theta_i'(H)$ after subtraction of these straight lines. The criterion for the selection of the “fitting” straight

line was the following conditions: the magneto-optical hysteresis loop is symmetric with respect to the origin of coordinates, and the linear section of the saturation magnetization is parallel to the ordinate axis. In the “fitting” equation, the direct free term $\Delta\Theta$ characterizes the effect of vertical displacement of the magneto-optical hysteresis loop and can be easily found in Equation (2), and the slope k characterizes the degree of loop deformation. It can be seen that the degree of magneto-optical hysteresis loop deformation is different in different spectrum areas. The maximum magneto-optical hysteresis loop deformation coefficient $k = -2.7 \times 10^{-4}$ deg/mT is observed at $\lambda = 640$ nm, and it decreases upon the wavelength increasing ($k = -2.4 \times 10^{-4}$ deg/mT at $\lambda = 750$ nm and $k = -2.25 \times 10^{-4}$ deg/mT at $\lambda = 920$ nm accordingly).

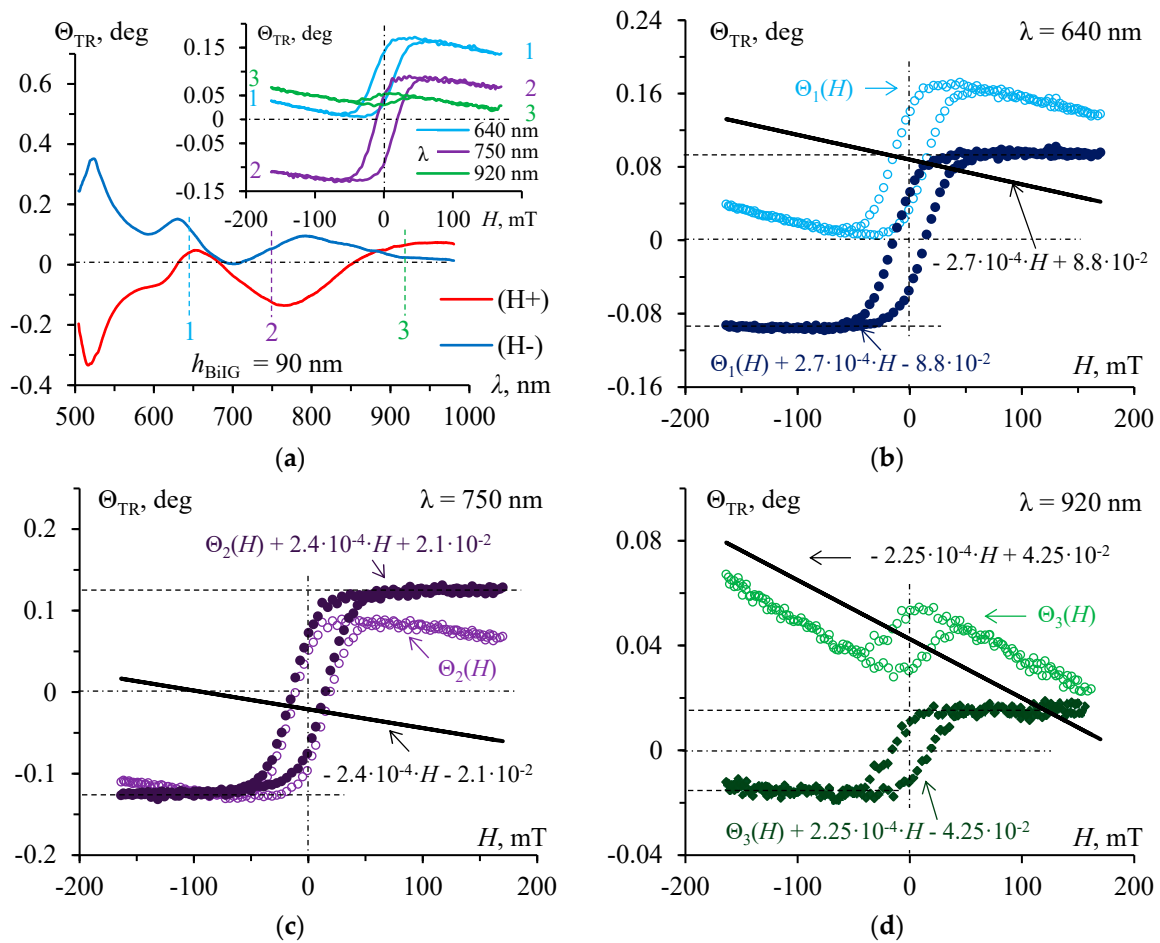


Figure 6. Results of the analysis of magneto-optical hysteresis loops, which is obtained at different values of the incident radiation wavelength λ for the GGG/Au_(NP)/BiIG_(grad h) sample with a thickness of $h_{BiIG} = 90$ nm. (a) Spectra of magneto-optical rotation in the fields $H+$ and $H-$ (dashed line and the numbers show the spectral ranges where the magneto-optical hysteresis loop was studied, inset shows the corresponding view of magneto-optical hysteresis loop); (b–d) analysis of displacement and deformation of magneto-optical hysteresis loops $\Theta_i(H)$ (empty circles—measured loop, filled circles—corrected loop, line—corrective straight line).

Analysis shows that after subtraction of the “fitting” straight line, the form of all magneto-optical hysteresis loops becomes the same up to a multiple factor, i.e., $a_1 \cdot \Theta_1'(H) = a_2 \cdot \Theta_2'(H) = a_3 \cdot \Theta_3'(H)$. This indicates that the nature of the magneto-optical hysteresis loop is identical and is due to the true Faraday Effect, taking into account the resonant amplification in the region of different LPR modes in the plasmon subsystem of the nanocomposite. The deformation of the magneto-optical hysteresis loop shape is associated with the paramagnetic contribution from the GGG substrate (rather thick relative to the magneto-optical BiIG layer).

4. Conclusions

The results of the design, synthesis, and investigation of spatially nonhomogeneous magnetoplasmonic nanocomposite GGG/Au_(NP)/BiIG_(grad h) are demonstrated in this work. The features of the interaction of a magnetoactive iron-garnet layer with various plasmon modes in self-assembled Au nanoparticles have been studied. It has been shown experimentally that an increase in the thickness of the magnetoactive matrix of the iron-garnet layer leads not only to a change in the LPR resonance frequency but also to a change in the efficiency of excitation of various resonance LPR modes.

An enhancement of the magneto-optical Faraday Effect in the spectral range of various LPR modes was found, with the activity of the dipole *d*-mode being significantly higher than the activity of the coupled *d-d*-mode (maximum of enhancement is more than 20 times for the plasmonic *d*-mode, and 1.5 times for the *d-d*-mode).

A clear correlation between the asymmetry of magneto-optical rotation (vertical shift of the magneto-optical hysteresis loop) and the spectrum of the derivative of transmittance was revealed. So, the spectral features of asymmetry of magneto-optical rotation are dependent on the position and width of the resonance lines of different LPR modes. It indicates the “plasmonic” nature of the appearance of this effect due to the enhancement of the near field around the plasmonic nanoparticle at the LPR condition. The nature of this asymmetric magneto-optical rotation is associated with the Cotton–Mouton effect when the magnetization of the garnet medium in the direction normal to the radiation wave vector appears due to the magnetic component of the near field of resonating nanoparticles.

An anomalous behavior has been found in the spectral dependences of the magneto-optical rotation $\Theta_{TR}(\lambda)$ in the GGG/Au_(NP)/BiIG_(grad h) nanocomposite (the intersection of spectral curves during magnetization of the sample in the inverse fields *H*+ and *H*-). It is shown that this phenomenon is associated with the shape deformation of the magneto-optical hysteresis loop due to the paramagnetic contribution of the GGG substrate and to the vertical displacement of the loop caused by the Cotton–Mouton effect.

Thus, the discovered effect of asymmetric magneto-optical rotation (vertical displacement of the magneto-optical hysteresis loop) in a magnetoplasmonic nanocomposite must be taken into account in designing and studying magnetoplasmonic structures of this type. This effect can potentially be used in photonic devices, such as photonic and magneto-photonic crystals, with tunable properties.

Author Contributions: Investigation and writing—original draft preparation, S.T.; investigation A.K.; investigation, S.L.; investigation, O.T.; supervision, V.B.; project administration, A.G.; visualization, W.L.; writing—review and editing, A.Y. All authors have read and agreed to the published version of the manuscript.

Funding: The research was financially supported by the Russian Science Foundation (grant No. 19-72-20154, <https://rscf.ru/project/19-72-20154/>, accessed on 1 June 2023).

Institutional Review Board Statement: Not applicable.

Informed Consent Statement: Not applicable.

Data Availability Statement: No new data were created.

Conflicts of Interest: The authors declare no conflict of interest. The funders had no role in the design of the study; in the collection, analyses, or interpretation of data; in the writing of the manuscript; or in the decision to publish the results.

References

1. Armelles, G.; Cebollada, A.; García-Martín, A.; González, M.U. Magnetoplasmonics: Combining Magnetic and Plasmonic Functionalities. *Adv. Opt. Mater.* **2013**, *1*, 10–35. [CrossRef]
2. Uchida, H.; Mizutani, Y.; Nakai, Y.; Fedyanin, A.A.; Inoue, M. Garnet composite films with Au particles fabricated by repetitive formation for enhancement of Faraday effect. *J. Phys. D Appl. Phys.* **2011**, *44*, 064014. [CrossRef]
3. Dotsch, H.; Hertel, P.; Luhrmann, B.; Sure, S.; Winkler, H.P.; Ye, M. Applications of magnetic garnet films in integrated optics. *IEEE Trans. Magn.* **1992**, *28*, 2979–2984. [CrossRef]

4. Yang, Y.; Liu, T.; Bi, L.; Deng, L. Recent advances in development of magnetic garnet thin films for applications in spintronics and photonics. *J. Alloys Compd.* **2021**, *860*, 158235. [[CrossRef](#)]
5. Dötsch, H.; Holthaus, C.; Trifonov, A.; Klank, M.; Hagedorn, O.; Shamonin, M.; Schützmann, J. Application of Magnetic Garnet Films for Magneto-optical Imaging of Magnetic Field Distributions. *MRS Proc.* **2004**, *834*, J6.1. [[CrossRef](#)]
6. Voronov, A.A.; Karki, D.; Ignatyeva, D.O.; Kozhaev, M.A.; Levy, M.; Belotelov, V.I. Magneto-optics of subwavelength all-dielectric gratings. *Opt. Exp.* **2020**, *28*, 17988. [[CrossRef](#)]
7. Voronov, A.A.; Ignatyeva, D.O.; Karki, D.; Kozhaev, M.A.; Kalish, A.N.; Levy, M.; Belotelov, V.I. Resonances of the Faraday Effect in Nanostructured Iron Garnet Films. *JETP Lett.* **2020**, *112*, 720–724. [[CrossRef](#)]
8. Uchida, H.; Masuda, Y.; Fujikawa, R.; Baryshev, A.V.; Inoue, M. Large enhancement of Faraday rotation by localized surface plasmon resonance in Au nanoparticles embedded in Bi:YIG film. *J. Magn. Magn. Mater.* **2009**, *321*, 843–845. [[CrossRef](#)]
9. Tkachuk, S.; Lang, G.; Krafft, C.; Rabin, O.; Mayergoyz, I. Plasmon resonance enhancement of Faraday rotation in thin garnet films. *J. Appl. Phys.* **2011**, *109*, 07B717. [[CrossRef](#)]
10. Mizutani, Y.; Uchida, H.; Masuda, Y.; Baryshev, A.V.; Inoue, M. Magneto-optical plasmonic Bi:YIG composite films with Ag and Au-Ag alloy particles. *J. Magn. Soc. Jpn.* **2009**, *33*, 481–484. [[CrossRef](#)]
11. Baryshev, A.V.; Uchida, H.; Inoue, M. Peculiarities of plasmon-modified magneto-optical response of gold-garnet structures. *J. Opt. Soc. Am. B* **2013**, *30*, 2371–2376. [[CrossRef](#)]
12. Fujikawa, R.; Baryshev, A.V.; Kim, J.; Uchida, H.; Inoue, M. Contribution of the surface plasmon resonance to optical and magneto-optical properties of a Bi:YIG-Au nanostructure. *J. Appl. Phys.* **2008**, *103*, 07D301. [[CrossRef](#)]
13. Amirjani, A.; Abyaneh, P.Z.; Masouleh, P.A.; Sadrnezhaad, S.K. Finite and Boundary Element Methods for Simulating Optical Properties of Plasmonic Nanostructures. *Plasmonics* **2022**, *17*, 1095–1106. [[CrossRef](#)]
14. Amirjani, A.; Sadrnezhaad, S.K. Computational electromagnetics in plasmonic nanostructures. *J. Mater. Chem. C* **2021**, *9*, 9791–9819. [[CrossRef](#)]
15. Ahmadvand, A.; Gerislioglu, B.; Ramezani, Z. Generation of magnetoelectric photocurrents using toroidal resonances: A new class of infrared plasmonic photodetectors. *Nanoscale* **2019**, *11*, 13108–13116. [[CrossRef](#)]
16. Yin, J.; Zang, Y.; Xu, B.; Li, S.; Kang, J.; Fang, Y.; Wu, Z.; Li, J. Multipole plasmon resonances in self-assembled metal hollow-nanospheres. *Nanoscale* **2014**, *6*, 3934–3940. [[CrossRef](#)]
17. Kumbhar, A.S.; Kinnan, M.K.; Chumanov, G. Multipole Plasmon Resonances of Submicron Silver Particles. *J. Am. Chem. Soc.* **2005**, *127*, 12444–12445. [[CrossRef](#)] [[PubMed](#)]
18. Raza, S.; Kadkhodazadeh, S.; Christensen, T.; Vece, M.; Wubs, M.; Mortensen, N.A.; Stenger, N. Multipole plasmons and their disappearance in few-nanometre silver nanoparticles. *Nat. Commun.* **2015**, *6*, 8788. [[CrossRef](#)]
19. Takayuki, U.; Tsuyoshi, A.; Hiroshi, M.; Daisuke, I.; Manabu, F.; Toshihiro, T. Multipole Resonance Modes in Localized Surface Plasmon of Single Hexagonal/Triangular Gold Nanoplates. *Chem. Lett.* **2007**, *36*, 318–319.
20. Khramova, A.E.; Ignatyeva, D.O.; Kozhaev, M.A.; Dagesyan, S.A.; Berzhansky, V.N.; Shaposhnikov, A.N.; Tomilin, S.V.; Belotelov, V.I. Resonances of the magneto-optical intensity effect mediated by interaction of different modes in a hybrid magnetoplasmonic heterostructure with gold nanoparticles. *Opt. Exp.* **2019**, *27*, 33170. [[CrossRef](#)]
21. Tomilin, S.V.; Berzhansky, V.N.; Shaposhnikov, A.N.; Lyashko, S.D.; Mikhailova, T.V.; Tomilina, O.A. Spectral Properties of Magneto-plasmonic Nanocomposite. Vertical Shift of Magneto-Optical Hysteresis Loop. *J. Phys. Conf. Ser.* **2019**, *1410*, 012122. [[CrossRef](#)]
22. Baryshev, A.V.; Merzlikin, A.M. Tunable Plasmonic Thin Magneto-Optical Wave Plate. *J. Opt. Soc. Am. B* **2016**, *33*, 1399. [[CrossRef](#)]
23. Harvey, B.M.; Spano, F.C. Theory of the Faraday effect with weak laser pulses. *J. Opt. Soc. Am. B* **1994**, *11*, 1177–1185. [[CrossRef](#)]
24. Tomilin, S.V.; Berzhansky, V.N.; Shaposhnikov, A.N.; Prokopov, A.R.; Karavaynikov, A.V.; Milyukova, E.T.; Mikhailova, T.V.; Tomilina, O.A. Vertical Displacement of the Magneto-optical Hysteresis Loop in the Magnetoplasmonic Nanocomposite. *Phys. Sol. State* **2020**, *62*, 144–152. [[CrossRef](#)]
25. Mikhailova, T.V.; Shaposhnikov, A.N.; Tomilin, S.V.; Alentiev, D.V. Nanostructures with magneto-optical and plasmonic response for optical sensors and nanophotonic devices. *J. Phys. Conf. Ser.* **2019**, *1410*, 012163. [[CrossRef](#)]
26. Satoshi, T.; Takeshi, K.; Shigeru, T.; Satoshi, I.; Minoru, F.; Shinji, H. Magneto-Optical Kerr Effects of Yttrium-Iron Garnet Thin Films Incorporating Gold Nanoparticles. *Phys. Rev. Lett.* **2006**, *96*, 167402.
27. Mejia-Salazar, J.R.; Camacho, S.A.; Constantino, C.J.L.; Oliveira, O.N. New trends in plasmonic (bio)sensing. *An. Acad. Bras. Cienc.* **2018**, *90*, 779–801. [[CrossRef](#)]
28. Tomilin, S.V.; Berzhansky, V.N.; Shaposhnikov, A.N.; Prokopov, A.R.; Milyukova, E.T.; Karavaynikov, A.V.; Tomilina, O.A. Ultrathin and Nanostructured Au Films with Gradient of Effective Thickness. Optical and Plasmonic Properties. *J. Phys. Conf. Ser.* **2016**, *741*, 012113. [[CrossRef](#)]
29. Kelly, K.L.; Coronado, E.; Zhao, L.L.; Schatz, G.C. The Optical Properties of Metal Nanoparticles: The Influence of Size, Shape, and Dielectric Environment. *J. Phys. Chem. B* **2003**, *107*, 668–677. [[CrossRef](#)]
30. Gao, R.; Chen, J.; Fan, G.; Jiao, W.; Liu, W.; Liang, C.; Ren, H.; Wang, Y.; Ren, S.; Wei, Q.; et al. Optical properties of formation of gold nanoparticle aggregates deposited on quartz glass and application to SPR sensing. *Opt. Mater.* **2022**, *125*, 112104. [[CrossRef](#)]
31. Tomilin, S.V.; Karavaynikov, A.V.; Lyashko, S.D.; Milyukova, E.T.; Tomilina, O.A.; Yanovsky, A.S.; Belotelov, V.I.; Berzhansky, V.N. Giant enhancement of the Faraday Effect in a magnetoplasmonic nanocomposite. *Opt. Mat. Exp.* **2022**, *12*, 1522–1530. [[CrossRef](#)]

32. Kreibig, U.; Volmer, M. *Optical Properties of Metal Clusters*; Springer: Berlin, Germany, 1995.
33. Tarasenko, S.V.; Shavrov, V.G. Additional Nonreciprocity Effects in the Magneto-Optics of Asymmetric Layer Structures. *JETP Lett.* **2018**, *108*, 384–390. [[CrossRef](#)]

Disclaimer/Publisher's Note: The statements, opinions and data contained in all publications are solely those of the individual author(s) and contributor(s) and not of MDPI and/or the editor(s). MDPI and/or the editor(s) disclaim responsibility for any injury to people or property resulting from any ideas, methods, instructions or products referred to in the content.